Proceedings of the 17th World Congress
The International Federation of Automatic Control
Seoul, Korea, July 6-11, 2008

On the optimal harmonic gait for locomotion of mechanical rectifier systems ⋆

J. Blair and T. Iwasaki

Mechanical and Aerospace Engineering, University of Virginia
122 Engineer's Way, Charlottesville, VA 22904 USA
e-mail: {jtb8s,iwasaki}@virginia.edu

Abstract: This paper formally defines a class of multibody rectifier systems that captures the essential aspects of animal locomotion, and formulates an optimal locomotion problem to find a set of harmonic inputs that minimizes a quadratic objective function subject to an equality constraint on the average velocity. Our main result shows that the global optimum is given in terms of a generalized eigenvalue of a pair of Hermitian matrices, with a minimizer characterized by the associated eigenvector. Thus, an optimal harmonic gait can be computed efficiently even for hyper-redundant rectifiers with a large number of variables. We provide case studies for two specific rectifiers; (i) a chain of multiple links mimicking snakes, leeches, and other slender animals, and (ii) a disk-mass system that captures the rectifying dynamics in the simplest way. We examine optimal gaits for three types of objective functions, consisting of input power, input torque, and shape derivative. We compare the multilink results against natural motions observed in leeches, and discuss what optimality criteria appear to be used in nature. Analytical results are obtained for the disk-mass system, providing insights into optimal gaits.

Keywords: Optimal Control; Animal Locomotion; Motion Planning; Gait; Mechanical Rectifier

1. INTRODUCTION

Animals use "gaits," or distinct sets of rhythmic body movements,to produce a nonzero average velocity through the interaction with their environment. Thus, animal locomotion can generally be viewed as mechanical rectification, converting rhythmic motion into a biased velocity. A fundamental control problem in the design of a robotic locomotor is to determine a gait that can generate a desired velocity for a given mechanical configuration. Clearly, there can be many gaits that satisfy the velocity constraint, and it is important to find the one that optimizes a quantity such as input power. Moreover, when the number of actuators is less than the number of shape variables, it is essential to ensure achievability of a gait through the given set of actuators.

Optimal gaits for robotic locomotors have been investigated in literature. One approach is based on biological inspirations, wherein a particular gait, observed in animal locomotion, is parameterized and examined for optimality with respect to a cost function. Optimizations are typically performed via gridding of the parameter space and numerical simulations. This type of approach has been taken to search for optimal gaits for robots that mimic human walking (Chevallereau and Aoustin, 2001), snake crawling (Saito et al., 2002), and anguilliform swimming (McIsaac and Ostrowski, 2003). Methods such as these might obtain an optimal parameter set within the particular gait examined, but may miss globally optimal gaits that differ from what is observed in biology.

Other approaches to find optimal gaits are based on some standard formulations of optimal control problems and various combinations of existing optimization methods. A popular method is to expand the signals over a finite set of basis functions, reducing the problem to a parametric optimization. Cortes et al. (2001) used this method to find an optimal gait for eel swimming, where the necessary condition for optimality was solved using Newton iteration. Saidouni and Bessonnet (2003) also used this method for biped walking with the aid of sequential quadratic programming. Another well known method is to apply the calculus of variations to reduce the optimization to a two-point boundary-value problem. This method has been used by Ostrowski et al. (2000) for nonholonomic locomotion systems, by Bessonnet et al. (2004) for a seven-link biped robot, and by Hicks and Ito (2005) for shape actuated locomotion systems. While it would be ideal to have global solutions to general optimal control problems, all of the existing methods solve conditions for local optimality. Hence, the solution depends on the initial condition of the numerical search in general, and hence can be far from the global optimum.

In this paper, we take a different approach. Instead of finding a locally optimal solution to a general locomotion problem, we provide a globally optimal solution to an approximate locomotion problem. In this way, potential nonoptimality is not hidden behind the numerical optimization procedure, but is explicit in the problem formulation. The process to compute the solution is fast and stable. Hence, our method can be applied to hyper-redundant rectifier systems with many degrees of freedom. Another advantage is that an optimal gait is found within those achievable by the given set of actuators. This feature is especially important for systems that have less actuators than the number of shape variables because not all gaits are achievable by a small number of actuators.

To this end, we first characterize a general class of dynamic rectifier systems that captures the essential aspects of animal locomotion, and then approximate the system by assuming small perturbations around a nominal posture. The resulting

⋆ This work is supported by NSF 0237708 and 0654070.

model extracts the rectifier dynamics as a bilinear term of the shape variables and their derivatives. An optimal locomotion problem is formulated for the bilinear rectifier where an integral quadratic function is minimized over the set of harmonic inputs, subject to an equality constraint on the average velocity. The problem is reduced to a finite dimensional, constrained, nonconvex quadratic optimization over the input phasor and frequency. We then show that the globally optimal solution can be found by calculating the generalized eigenvalues of a pair of Hermitian matrices and by sweeping over the frequency.

We provide two case studies. One is undulatory locomotion of a chain of multiple links, which is a model for snake crawling or leech/lamprey swimming. We find optimal gaits that minimize the input power, input torque, or shape derivative, and compare with an observed motion in biology. The other is a disk-mass system that captures the rectifier dynamics in the simplest manner. Analytical solutions are obtained for this simple case, which is used to make some general observations through analogy to more complex rectifiers.

2. RECTIFIER SYSTEMS

The following sections describe the general equations of motion, their approximations, and specific examples.

2.1 General equations of motion

Consider the class of multilink systems given by

$$\begin{aligned} &J_\theta\ddot{\theta} + G_\theta\dot{\theta}^2 + R_\theta^\mathsf{T}\gamma(R_\theta\dot{\theta} + N_\theta v) = Bu, \\ &m\dot{v} + N_\theta^\mathsf{T}\gamma(R_\theta\dot{\theta} + N_\theta v) = 0, \end{aligned} \tag{1}$$

where $\theta(t) \in \mathbb{R}^n$ are the link angles, $v(t) \in \mathbb{R}^k$ is the velocity of the center of gravity, $u(t) \in \mathbb{R}^\ell$ are the torque inputs at selected joints, and $\dot{\theta}^2$ denotes the vector whose i^{th} entry is $\dot{\theta}_i^2$. The coefficient matrices J_θ, G_θ, R_θ, and N_θ depend on θ, and m is the total mass of the system. The terms $J_\theta\ddot{\theta} + G_\theta\dot{\theta}^2$ are standard in multilink systems. The terms involving $\gamma(\cdot)$ are related to the interactive forces (and torques) from the surrounding environment, such as frictions and fluid forces, as well as damping effects at the body joints. The quantity $R_\theta\dot{\theta} + N_\theta v$ is the vector of relative velocities on which the interactive forces depend, and the function $\gamma : \mathbb{R}^p \to \mathbb{R}^p$ is a possibly nonlinear, diagonal mapping that generates the force resulting from the relative motion. Each diagonal entry of γ typically satisfies the sector condition $\gamma_i(x)x > 0$ for nonzero x.

This class of systems captures the essential dynamics of animal locomotion with continuous interactions with the environment. For instance, the dynamics of snake crawling, leech and manta ray swimming, and possibly flapping flight of birds and insects are captured by (1). Roughly speaking, the first equation in (1) describes how the body shape θ changes in response to the joint torque input u, while the second governs how the local shape change θ translates into the global velocity v through the interaction with the environment. The intended operation of the system is *locomotion*, that is, a sustained steady forward velocity v through rhythmic body movements. We call such systems *mechanical rectifiers* as they convert periodic torque (or force) inputs to a biased velocity.

We assume that the system (1) possesses a *nominal posture* $\eta \in \mathbb{R}^n$, which satisfies

$$R_\eta^\mathsf{T}\gamma(N_\eta v) = 0, \quad N_\eta^\mathsf{T}\gamma(N_\eta v) \in \mathbb{V}, \quad \forall\, v \in \mathbb{V},$$

where $\mathbb{V}$ is a straight line in $\mathbb{R}^k$ indicating the direction of locomotion. This means that a body starting from a nominal posture with velocity $v \in \mathbb{V}$ would keep its body shape and direction of locomotion when there is no input u. The line $\mathbb{V}$ often coincides with the axis of symmetry for the multilink body. For instance, a nominal posture for a snake is a straight configuration and $\mathbb{V}$ is the line containing the body. Without loss of generality, we assume that $\mathbb{V}$ is aligned with the vector $e_1 \in \mathbb{R}^k$ whose first entry is one and the rest are zeros.

We attempt to analyze the behavior of the original system (1) through an approximate model that is simple enough to give insights for, and yet captures the essential dynamics of, mechanical rectification. To this end, we restrict our attention to those systems for which it is reasonable to approximate the interactive force by a linear function (through such methods as standard linearization and describing function), i.e., $\gamma(x) \cong \Gamma x$ for a constant matrix Γ. Furthermore, we consider small amplitude oscillation about a nominal posture $\vartheta := \theta - \eta$, and exploit the following approximations:

$$\begin{aligned} &J_\theta = J + \mathsf{O}(\vartheta), \quad R_\theta^\mathsf{T}\Gamma R_\theta = D + \mathsf{O}(\vartheta), \\ &R_\theta^\mathsf{T}\Gamma N_\theta = E(\vartheta) + \mathsf{O}(\vartheta^2), \quad N_\theta^\mathsf{T}\Gamma N_\theta = C(\vartheta) + \mathsf{O}(\vartheta^3), \end{aligned}$$

where J and D are constant, $E(\vartheta)$ and $C(\vartheta)$ are first and second order in ϑ, respectively. By the definition of a nominal posture, we have $E(0)e_1 = 0$ and $C(0)e_1 \in \mathbb{V}$. For simplicity, we assume that $E(\vartheta)w = 0$ for all $\vartheta \in \mathbb{R}^n$ and w in the orthogonal complement of $\mathbb{V}$, which is satisfied for the particular rectifier systems described in the next subsections. The function $E(\vartheta)$ can then be expressed as $E(\vartheta) = [\,\Lambda\vartheta\ 0\,]$ for some square *asymmetric* matrix Λ. We now linearize the first equation in (1) in terms of ϑ. However, we choose not to linearize the second equation as the essential mechanism of rectification will be lost by such approximation. Instead, we keep up to the second order terms in ϑ. With these approximations, the original system (1) reduces to the following:

$$\begin{aligned} &J\ddot{\vartheta} + D\dot{\vartheta} + v_1\Lambda\vartheta = Bu, \\ &m\dot{v} + C(\vartheta)v + e_1(\dot{\vartheta}^\mathsf{T}\Lambda\vartheta) = 0, \end{aligned} \tag{2}$$

where $v_1 := e_1^\mathsf{T}v$ is the locomotion speed.

This model appears to be the simplest model to capture the essential dynamics of the mechanical rectifier. The fundamental component of the rectifying dynamics can be captured by a bilinear term of the form $\dot{\vartheta}^\mathsf{T}\Lambda\vartheta$, but not by a linear term. In particular, the integral of $\dot{\vartheta}^\mathsf{T}\Lambda\vartheta$ over one cycle is nonzero due to the asymmetry of Λ, so that periodic body movements can generate a thrust for locomotion. The dynamics of the body oscillations is captured by a linear model with the slowly time-varying, asymmetric stiffness matrix $v_1\Lambda$ that depends on the locomotion speed v_1.

2.2 Undulatory locomotor

This section describes an example of rectifier systems. The body of slender animals that undulate for locomotion, such as crawling snake (Hirose, 1993; Saito et al., 2002), and swimming leech and lamprey (Bowtell and Williams, 1991; Ekeberg, 1993), can be modeled by a chain of n rigid links as shown in Fig. 1. The undulatory motions are typically in a plane ($k = 2$), e.g., horizontal plane for snakes and vertical plane for leeches. The body is free to move in the plane and is actuated at every joint by torque input $u \in \mathbb{R}^\ell$ with $\ell = n - 1$.

The key property for mechanical rectification is the difference in the tangential and normal components of the interactive force from the environment acting on each link. In particular, the normal force tends to be much larger than the tangential force. This is true for snake crawling on the ground (Hirose, 1993) as well as for slender-body swimming (Taylor, 1952; McMillen and Holmes, 2006). The simplest way to capture this property, which is often adequate for at least qualitative analyses, is to approximate the tangential and normal forces on each link (f_{t_i} and f_{n_i}) by linear functions of the respective components of the relative velocity between the link and environment (v_{t_i} and v_{n_i}). That is, for the i^{th} link,

$$f_{t_i} = c_{t_i} v_{t_i}, \quad f_{n_i} = c_{n_i} v_{n_i}, \tag{3}$$

where c_{t_i} and c_{n_i} are constants such that $c_{t_i} \ll c_{n_i}$.

The equations of motion for the link chain subject to the environmental force (3) are given by (1) with the definitions (Saito et al., 2002)

$$J_\theta := J + S_\theta H S_\theta + C_\theta H C_\theta, \quad G_\theta := S_\theta H C_\theta - C_\theta H S_\theta,$$
$$R_\theta := \begin{bmatrix} \Omega_\theta L_\theta \\ I \end{bmatrix}, \quad N_\theta := \begin{bmatrix} \Omega_\theta E \\ 0 \end{bmatrix}, \quad m := \sum_{i=1}^{n} m_i,$$
$$L_\theta := \begin{bmatrix} F S_\theta \\ -F C_\theta \end{bmatrix}, \quad \Omega_\theta := \begin{bmatrix} C_\theta & S_\theta \\ -S_\theta & C_\theta \end{bmatrix}, \quad E := \begin{bmatrix} e & 0 \\ 0 & e \end{bmatrix},$$
$$S_\theta := \mathrm{diag}(\sin\theta_1, \ldots, \sin\theta_n), \quad e := [\, 1 \ \ldots \ 1 \,]^{\mathsf{T}} \in \mathbb{R}^n,$$
$$C_\theta := \mathrm{diag}(\cos\theta_1, \ldots, \cos\theta_n), \quad J := \mathrm{diag}(J_1, \ldots, J_n),$$
$$H := LA(B^{\mathsf{T}} M^{-1} B)^{-1} A^{\mathsf{T}} L, \quad M := \mathrm{diag}(m_1, \ldots, m_n),$$
$$F := M^{-1} B (B^{\mathsf{T}} M^{-1} B)^{-1} A^{\mathsf{T}} L, \quad L := \mathrm{diag}(\ell_1, \ldots, \ell_n),$$
$$C_t := \mathrm{diag}(c_{t_1}, \ldots, c_{t_n}), \quad C_n := \mathrm{diag}(c_{n_1}, \ldots, c_{n_n}),$$
$$\gamma(x) := \Gamma x, \quad \Gamma := \mathrm{diag}(C_t, C_n, C_n L^2/3),$$
$$A := \begin{bmatrix} 1 & 1 & & \\ & \ddots & \ddots & \\ & & 1 & 1 \end{bmatrix}^{\mathsf{T}}, \quad B := \begin{bmatrix} 1 & -1 & & \\ & \ddots & \ddots & \\ & & 1 & -1 \end{bmatrix}^{\mathsf{T}},$$

where $A, B \in \mathbb{R}^{n\times(n-1)}$, $\theta \in \mathbb{R}^n$, $u \in \mathbb{R}^{n-1}$, and $v \in \mathbb{R}^2$.

To focus on the essential dynamics, we consider the case where the links are identical; $m_i = m_o$, $\ell_i = \ell_o$, $J_i = J_o := m_o \ell_o^2/3$, $c_{t_i} = c_t$, and $c_{n_i} = c_n$ for all i. We set the nominal posture η to be zero. Assuming that the perturbation of θ from the nominal posture is small in amplitude, the equations of motion become of the form given by (2) with the definitions

$$J := J_o I + H, \quad D := c_n (F^{\mathsf{T}} F + (\ell_o^2/3) I)$$
$$\Lambda := (c_n - c_t) F^{\mathsf{T}}, \quad C(\vartheta) := \begin{bmatrix} n c_t + c_n \vartheta^{\mathsf{T}} \vartheta & (c_t - c_n) e^{\mathsf{T}} \vartheta \\ (c_t - c_n) e^{\mathsf{T}} \vartheta & n c_n + c_t \vartheta^{\mathsf{T}} \vartheta \end{bmatrix}.$$

As noted earlier, the propulsive force due to rhythmic body movements is captured by the term $\dot\vartheta^{\mathsf{T}} \Lambda \vartheta$ in (2). If $c_n = c_t$, then no such force is generated and no undulation pattern leads to locomotion. If $c_n \gg c_t$ as in many animals, nonzero net momentum is generated over one cycle due to asymmetry of Λ.

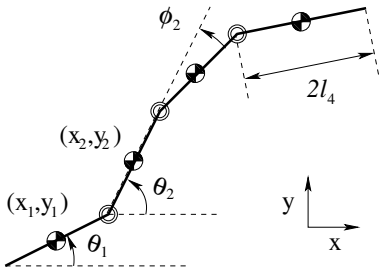

Fig. 1. Multilink chain system

2.3 Simple mechanical rectifier

A very simple model, as shown in Fig. 2, which consists of a spinning disk with moment of inertia J, driven by the friction of a point mass m sliding on its surface, contains all the essential elements of the locomotion problem. The point mass receives a controlling force u and represents the dynamics of an organisms body. The friction force between point mass and disk, which is proportional to the relative velocity with constant c, represents the interaction of the body with the environment, and the angular velocity of the disk ϖ represents the locomotion speed. We call this system a simple mechanical rectifier (SMR) since periodic movements of the mass can be rectified to yield disk rotation in a fixed direction on average.

The equation of motion is given by

$$\begin{aligned} &m\ddot\rho + (c+d)\dot\rho + c\varpi S\rho = u, \\ &J\dot\varpi + (a + c\rho^{\mathsf{T}}\rho)\varpi + c\dot\rho^{\mathsf{T}} S\rho = 0, \end{aligned} \tag{4}$$

where $\rho(t) \in \mathbb{R}^2$ is the coordinate of the point mass, and

$$S := \begin{bmatrix} 0 & 1 \\ -1 & 0 \end{bmatrix}.$$

The $d\dot\rho$ term represents the energy loss associated with the actuation of the point mass by input u, and $a\varpi$ is the frictional torque at the disk bearing. Clearly, (4) is of the form (2) where ρ and ϖ correspond to ϑ and v, respectively. Note that the nominal posture ($\rho = 0$) for SMR is when the mass is at the disk center.

To examine the mechanism of rectification, let us consider the case where the disc inertia J is so large that ϖ may be considered constant over a cycle. In this case, the standard averaging technique yields

$$\varpi \cong \alpha \Big/ \int_0^T (a/c + \|\rho\|^2) dt,$$
$$\alpha := -\int_0^T \dot\rho^{\mathsf{T}} S\rho \, dt = \int_0^T (\rho_1\dot\rho_2 - \rho_2\dot\rho_1) dt,$$

where T is the cycle period of the mass movement. Note that α is a half of the area enclosed by the orbit of the mass trajectory $\rho(t)$, which is defined positive when the orbit goes counter-clockwise. For the same size of mass motion as measured by α, faster rotation is achieved if the mass motion occurs near the disk center so that ρ, and hence the denominator, is small. For this reason, it makes sense to choose the nominal posture at the disk center. The term $\rho_1\dot\rho_2 - \rho_2\dot\rho_1$ is the Lie bracket $[\rho_1, \rho_2]$, representing a canonical form of rectifying dynamics studied by Brockett (2003) in the context of nonholonomic systems control.

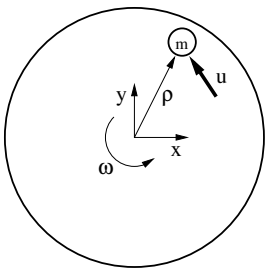

Fig. 2. Simple mechanical rectifier

3. OPTIMAL LOCOMOTION

In this section, we formulate an optimal locomotion problem for the mechanical rectifier (2) and provide a solution.

3.1 Problem formulation

We consider the optimal locomotion problem of minimizing a quadratic cost function over the set of T-periodic signals $\mathbb{S}_T$, subject to the constraint that the average speed of locomotion is v_o. The problem is formulated as

$$\min_{\substack{T\in\mathbb{R}_+\\ v,\vartheta,u\in\mathbb{S}_T}} \frac{1}{T}\int_0^T \begin{bmatrix}\dot\vartheta\\ u\end{bmatrix}^{\mathsf T}\Pi\begin{bmatrix}\dot\vartheta\\ u\end{bmatrix}dt \quad \text{s.t.} \quad \begin{cases} \dfrac{1}{T}\displaystyle\int_0^T v dt = v_o e_1,\\ J\ddot\vartheta + D\dot\vartheta + v_1\Lambda\vartheta = Bu,\\ m\dot v + C(\vartheta)v + (\dot\vartheta^{\mathsf T}\Lambda\vartheta)e_1 = 0, \end{cases} \tag{5}$$

where Π is a given symmetric matrix.

The objective function is quadratic in $\dot\vartheta$ and u, and has many physical interpretations depending on the choice of Π. Some possible physical quantities captured in this framework include input power, input torque, and rate of body shape change, and are summarized in the table below, where $\phi := B^{\mathsf T}\theta$ is the vector of relative link angles. The average value over one period is taken for input power, and mean-square values for the other two quantities. The method for solving the problem, presented below, can readily be extended to include ϑ terms in the quadratic objective function, but we choose not to do so for brevity.

Table 1. Objective functions specified by Π

Quantity	Objective Integral	Π
Input Power	$\frac{1}{T}\int_0^T \dot\phi^{\mathsf T}u dt$	$\frac{1}{2}\begin{bmatrix}0 & B\\ B^{\mathsf T} & 0\end{bmatrix}$
Input Torque	$\frac{1}{T}\int_0^T \|u\|^2 dt$	$\begin{bmatrix}0 & 0\\ 0 & I\end{bmatrix}$
Shape Change Rate	$\frac{1}{T}\int_0^T \|\dot\phi\|^2 dt$	$\begin{bmatrix}BB^{\mathsf T} & 0\\ 0 & 0\end{bmatrix}$

For tractability, we shall reformulate the problem in (5) by restricting the underlying class of periodic signals and approximating some constraints. In particular, the search for the optimal gait is confined to the class of T-periodic, unbiased, harmonic signals $\mathbb{H}_T$. Assuming that the dynamics of v is much slower than ϑ, we take the average of the third constraint in (5) over one cycle, with v regarded as constant. Solving for v, equating the result with the target velocity $v_o e_1$, and rearranging, we have

$$\int_0^T \Big(C(\vartheta)e_1 v_o + (\dot\vartheta^{\mathsf T}\Lambda\vartheta)e_1\Big)\,dt = 0.$$

The second row block (of dimension $k-1$) of this vector constraint is approximately satisfied due to the defining properties of the nominal posture and the small ϑ assumption. Hence, we consider only the first row of the constraint. The problem is now reformulated as

$$\min_{\substack{T\in\mathbb{R}_+\\ \vartheta,u\in\mathbb{H}_T}} \frac{1}{T}\int_0^T \begin{bmatrix}\dot\vartheta\\ u\end{bmatrix}^{\mathsf T}\Pi\begin{bmatrix}\dot\vartheta\\ u\end{bmatrix}dt \quad \text{s.t.} \quad \begin{cases} \displaystyle\int_0^T \Big(\mathsf{c}(\vartheta)v_o + \dot\vartheta^{\mathsf T}\Lambda\vartheta\Big)\,dt = 0,\\ J\ddot\vartheta + D\dot\vartheta + v_o\Lambda\vartheta = Bu \end{cases} \tag{6}$$

where $\mathsf{c}(\vartheta) := e_1^{\mathsf T}C(\vartheta)e_1$.

3.2 Harmonic solution

This section presents an exact solution to the problem in (6). The following lemma reduces the problem to a constrained quadratic optimization.

Lemma 1. Consider the minimization problem given by (6). Let the quadratic function $\mathsf{c}(\vartheta)$ be expressed as $\mathsf{c}(\vartheta) = \vartheta^{\mathsf T}\mathsf{C}\vartheta + \mathsf{b}^{\mathsf T}\vartheta + \mathsf{a}$ and define

$$\begin{aligned} X_\omega &:= \begin{bmatrix} j\omega P_\omega\\ I\end{bmatrix}^* \Pi \begin{bmatrix} j\omega P_\omega\\ I\end{bmatrix},\\ Y_\omega &:= P_\omega^*\left(j(\omega/v_o)(\Lambda-\Lambda^{\mathsf T}) - 2\mathsf{C}\right)P_\omega/(4\mathsf{a}),\\ P_\omega &:= (v_o\Lambda + j\omega D - \omega^2 J)^{-1}B. \end{aligned} \tag{7}$$

Then the problem is equivalent to

$$\min_{\omega\in\mathbb{R},\ \hat u\in\mathbb{C}^\ell} \{\ \hat u^* X_\omega \hat u :\ \hat u^* Y_\omega \hat u = 1\ \}. \tag{8}$$

In (8), the vector $\hat u$ is the phasor of the input signal $u(t)$. Hence, once (8) is solved for a minimizer $(\omega,\hat u)$, the optimal sinusoidal input for (6) can be found as $u(t) = \Re[\hat u e^{j\omega t}]$. To solve the problem in (8), one may optimize over $\hat u$ for a fixed ω, and repeat this process for various values of ω, numerically sweeping the frequency axis. In this case, each problem for a given ω is a static quadratic optimization, which is nonconvex in general because X_ω and Y_ω are possibly indefinite. Nonconvex optimizations are often hard to solve, but for this particular problem, we have a complete solution.

Lemma 2. Let Hermitian matrices X and Y be given and consider

$$\min_{q\in\mathbb{C}^\ell} \{\ q^*Xq :\ q^*Yq = 1\ \}. \tag{9}$$

The constraint is feasible if and only if the largest eigenvalue of Y is positive. In this case, the objective function is bounded below on the feasible set if and only if the following (convex) set is nonempty:

$$\mathbb{L} := \{\ \lambda\in\mathbb{R} :\ X \geq \lambda Y\ \}.$$

The largest element λ_o of $\mathbb{L}$ is well defined and is a generalized eigenvalue of (X,Y). The minimum value of (9) is equal to λ_o. An optimizer q_o is given by an eigenvector of the pair (X,Y) associated with the generalized eigenvalue λ_o, normalized so that $q_o^*Yq_o = 1$.

Based on Lemma 2, a solution to (9) can be found by computing the generalized eigenvalues of (X,Y). If the constraint is feasible and objective function is bounded, then one (or more) of the generalized eigenvalues must be real and satisfy $X \geq \lambda Y$. The largest of such generalized eigenvalues is λ_o. If λ_o is not repeated, then it has one-dimensional eigenspace. In this case, every eigenvector q_o satisfies $q_o^*Yq_o > 0$ and hence can be normalized so that $q_o^*Yq_o = 1$. This q_o is an optimizer of (9). If λ_o is repeated, then the dimension of the eigenspace is more than one and $q_o^*Yq_o$ can be nonpositive for some eigenvector.

However, Lemma 2 guarantees that at least one of them gives positive $q_o^* Y q_o$ and hence is a solution after the normalization.

Combining Lemmas 1 and 2, we immediately have the following result that solves the problem in (6).

Theorem 3. Consider the rectifier system given in (2) and the optimal locomotion problem in (6). Define X_ω, Y_ω, and P_ω by (7). Let σ be the optimal value of the objective function. Then we have

$$\sigma = \min_{\omega \in \mathbb{R}} \max_{\lambda \in \mathbb{R}} \{ \lambda : X_\omega \geq \lambda Y_\omega \}. \tag{10}$$

Let ω_o and λ_o be the optimizers. Then, the optimal period is $T = 2\pi/\omega_o$, and the optimal input and body angles are given by

$$u(t) = \Re[q_o e^{j\omega_o t}], \quad \vartheta(t) = \Re[P_{\omega_o} q_o e^{j\omega_o t}],$$

where $q_o \in \mathbb{C}^\ell$ is an eigenvector of the pair $(X_{\omega_o}, Y_{\omega_o})$ associated with the generalized eigenvalue λ_o, normalized to satisfy $q_o^* Y_{\omega_o} q_o = 1$.

The problem in (10) can be solved by generalized eigenvalue computation plus a line search. In particular, for a fixed ω, the solution λ to the maximization is given in terms of a generalized eigenvalue of (X, Y) as described in the paragraph below Lemma 2. Sweeping over ω by gridding the frequency axis, we have an optimal solution.

4. CASE STUDIES

The following subsections illustrate the optimal locomotions for specific examples.

4.1 Undulatory locomotor

We use the system given by (2) with parameter definitions in Section 2.2 to model leech swimming behavior. A leech swims by undulating its slender body in a vertical plane, propagating waves from head to tail just like crawling snakes. Based on experimental data of a medium size leech (Chen and Friesen, 2007), the model parameters are fixed as follows:

$$n = 18, \quad v_o = -0.157\,\mathrm{m/s}, \quad m = 0.0011\,\mathrm{kg},$$
$$\ell = 0.1073\,\mathrm{m}, \quad c_n = 0.8\ell_o\,\mathrm{N \cdot s/m}, \quad c_t = 0.1\ell_o\,\mathrm{N \cdot s/m},$$

where n is the number of links used for modeling, v_o is the observed average swim speed (negative sign indicates that the leech swam to the left), m and ℓ are the total mass and length, c_n and c_t are the drag coefficients for the tangential and normal fluid forces, and $\ell_o := \ell/(2n)$ and $m_o := m/n$. The leech body has a slightly larger density than water, but we assume for simplicity that it is neutrally buoyant.

We have solved the optimal locomotion problem in (6) with the objective functions summarized in Table 1. For each case, the problem is reformulated as in (8). Figure 3 shows the minimum of $\hat{u} X_\omega \hat{u}$ over $\hat{u}$ satisfying $\hat{u} Y_\omega \hat{u} = 1$, as a function of the frequency ω. Each function turned out to be quasi-convex and have a unique global minimum, for this particular example. The optimal undulation frequencies are found to be 25.6 rad/s (power), 86.9 rad/s (torque), and 21.2 rad/s (shape), whereas the frequency observed for the particular leech used for modeling was 17.0 rad/s.

The optimal body shapes are shown in Fig. 4. During swimming, the live leech exhibited about 250^o phase lag from head to tail, and roughly uniform (but slightly increasing toward the tail) amplitudes over the body around 10^o. The resulting body shape was fairly close to the one for the minimum shape derivative depicted in Fig. 4. Hence, it is tempting to conclude that the shape derivative, rather than the power or torque, may be closely related to the quantity that actual leeches minimize. However, the SMR example in the next subsection indicates that more careful examinations would be necessary before reaching such a conclusion.

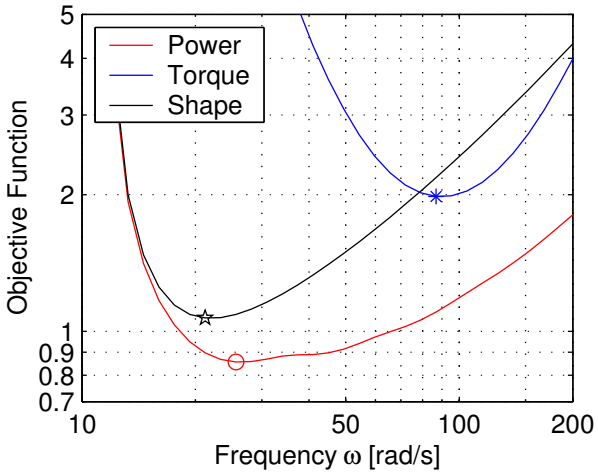

Fig. 3. Objective function vs. frequency ω: power in mW, torque in $(\mathrm{g{\cdot}mm})^2$, shape derivative in $(\mathrm{deg/ms})^2$.

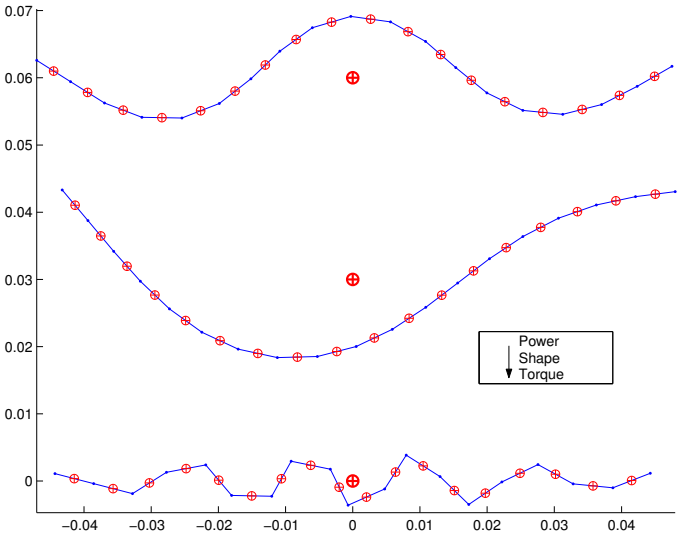

Fig. 4. Optimal body shapes (snapshots during swimming at an arbitrary time instant)

4.2 Simple mechanical rectifier

We shall apply Theorem 3 to the simple mechanical rectifier described by (4) to find two optimal gaits that minimize the input power and shape derivative, respectively, while maintaining the average angular velocity ϖ_o. In particular, we consider

$$\sigma := \min_{\substack{T \in \mathbb{R}_+ \\ \rho,\, u \in \mathbb{H}_T}} \frac{1}{T} \int_0^T f(\dot{\rho}, u) dt$$
$$\text{s.t.} \quad \begin{cases} \displaystyle\int_0^T \left((a + c\rho^{\mathsf{T}}\rho)\varpi_o + c\dot{\rho}^{\mathsf{T}} S \rho \right) dt = 0, \\ m\ddot{\rho} + (c+d)\dot{\rho} + \varpi_o c S \rho = u, \end{cases} \tag{11}$$

where $f(\dot{\rho}, u) := \dot{\rho}^{\mathsf{T}} u$ (input power) or $\|\dot{\rho}\|^2$ ("shape" derivative). The result is summarized as follows.

Proposition 4. Consider the simple mechanical rectifier in (4) and the optimal locomotion problem in (11). The globally optimal solution is characterized by

$$\rho(t) = \alpha \begin{bmatrix} \cos \omega t \\ \sin \omega t \end{bmatrix},$$

where ρ, α, and associated optimal cost σ, are given by Table 2 with $a_c := a/c$ and $d_c := d/c$.

Table 2. Optimal parameters for SMR locomotion

	Input Power	Shape Derivative
σ	$2ad_c\left(1+\sqrt{1+\frac{1}{d_c}}\right)^2 \varpi_o^2$	$8a_c\varpi_o^2$
α	$\sqrt{a_c\sqrt{1+\frac{1}{d_c}}}$	$\sqrt{a_c}$
ω	$\left(1+\sqrt{\frac{d_c}{1+d_c}}\right)\varpi_o$	$2\varpi_o$

The optimal orbit of the mass, $\rho(t)$, is circular; $\rho_1(t)$ and $\rho_2(t)$ have the same amplitude, and the former leads the latter by 90^o. This property is independent of the system parameters and the desired speed ϖ_o, but is determined by the structure of the rectifying dynamics as an eigenvector of S. In the general context, this suggests that the most fundamental mechanism for optimal gait selection is embedded in the eigenvectors of $\mathsf{S} := (\Lambda - \Lambda^{\mathsf{T}})/2$. More specifically, the eigenvector of $j\mathsf{S}$ associated with the maximum eigenvalue determines the basic gait, which maximizes the average propulsion over one cycle

$$\frac{1}{T}\int_0^T (-\dot{\vartheta}^{\mathsf{T}}\Lambda\vartheta)dt = j\omega\hat{\vartheta}^*\mathsf{S}\hat{\vartheta}/2$$

for given frequency ω and amplitude $\|\hat{\vartheta}\|$.

We notice from Table 2 that the optimal frequency ω is proportional to the desired speed ϖ_o, which makes physical sense. On the other hand, the optimal amplitude α is independent of ϖ_o, but scales with the square root of a/c. The parameters a and c roughly correspond to c_t and c_n in the undulatory locomotor, respectively. Hence, the fact that the ρ orbit is larger when a/c is larger, is analogous, for instance, to the fact that snakes undulate with larger amplitude on ice than on grounds.

Finally, we note that the optimal α and ω for the minimum input power approach that for the minimum shape derivative as d/c tends to infinity. If the cost (power loss) for the mass motion itself is much larger than the cost for driving the disk, then the minimum power gait tends to minimize the mass motion. Generalizing the idea for the undulatory locomotor, we expect that the optimal gaits from the input power and shape derivative minimizations would become similar if the joint frictions (ignored in our study) were large. In fact, this expectation turned out to be true, and moreover, optimal gaits from input torque minimization also approached the optimal shape derivative case. Thus, the choice of the objective functions among those in Table 1 is not important and all cases give similar results when the joint frictions are large.

5. CONCLUSION

We have formulated a locomotion problem for a class of mechanical rectifier systems to search for an optimal gait to achieve a given speed of locomotion on average. The problem is reduced to a generalized eigenvalue problem with frequency sweep, which can be solved efficiently. Unlike most, if not all, of existing approaches, our result provides a globally optimal solution. The key is not to compromise the solution by aiming for local optimality, but to reformulate the problem for tractability, in terms of a simplified model capturing the essential rectifier dynamics, with a restriction to harmonic driving inputs. The optimal harmonic gait thus obtained can be used as a reference signal for closed-loop control. Moreover, it can also be used, if desired, as an initial condition for the existing local algorithms to refine the gait for a more complex, fully nonlinear model of the rectifier dynamics.

ACKNOWLEDGEMENTS

The authors thank Professor W.O. Friesen and Ms. J. Chen for providing the motion data for a leech during swimming.

REFERENCES

G. Bessonnet, S. Chesse, and P. Sardain. Optimal gait synthesis of a seven-link planar biped. *The International journal of robotics research*, 23(10-11):1059–1073, 2004.

G. Bowtell and T.L. Williams. Anguilliform body dynamics: modeling the interaction between muscle activation and body curvature. *Phil. Trans. R. Soc. Lond. B*, 334:385–390, 1991.

R.W. Brockett. Pattern generation and the control of nonlinear systems. *IEEE Trans. Auto. Contr.*, 48(10):1699–1711, 2003.

J. Chen and W.O. Friesen. (personal communication). *University of Virginia*, 2007.

C. Chevallereau and Y. Aoustin. Optimal reference trajectories for walking and running of a biped robot. *Robotica*, 19:557–569, 2001.

J. Cortes, S. Martinez, J.P. Ostrowski, and K.A. McIsaac. Optimal gaits for dynamic robotic locomotion. *The International journal of robotics research*, 20(9):707–728, 2001.

O. Ekeberg. A combined neuronal and mechanical model of fish swimming. *Biological Cybernetics*, 69(5/6):363–374, 1993.

G. Hicks and K. Ito. A method for determination of optimal gaits with application to a snake-like serial-link structure. *IEEE Trans. Auto. Contr.*, 50(9):1291–1306, 2005.

S. Hirose. *Biologically Inspired Robots: Snake-Like Locomotors and Manipulators*. Oxford University Press, 1993.

K.A. McIsaac and J.P. Ostrowski. Motion planning for anguilliform locomotion. *IEEE Trans. Robotics and Automation*, 19(4):637–652, 2003.

T. McMillen and P. Holmes. An elastic rod model for anguilliform swimming. *J. Math. Biol.*, 53(5):843–886, 2006.

J.P. Ostrowski, J.P. Desai, and V. Kumar. Optimal gait selection for nonholonomic locomotion systems. *The International journal of robotics research*, 19:225–237, 2000.

T. Saidouni and G. Bessonnet. Generating globally optimised sagittal gait cycles of a biped robot. *Robotica*, 21(2), 2003.

M. Saito, M. Fukaya, and T. Iwasaki. Serpentine locomotion with robotic snake. *IEEE Control Systems Magazine*, 22(1): 64–81, 2002.

G. Taylor. Analysis of the swimming of long and narrow animals. *Proc. Royal Society of London. Series A*, 214(1117): 158–183, 1952.